Available online at www.sciencedirect.com

SCIENCE DIRECT

ELSEVIER

Palaeogeography, Palaeoclimatology, Palaeoecology 235 (2006) 245–264

PALAEO

www.elsevier.com/locate/palaeo

The late Hauterivian Faraoni oceanic anoxic event in the western Tethys: Evidence from phosphorus burial rates

Stéphane Bodin [a,*], Alexis Godet [a], Karl B. Föllmi [a], Jean Vermeulen [b], Hubert Arnaud [c], André Strasser [d], Nicolas Fiet [e], Thierry Adatte [a]

[a] Institut de Géologie, Université de Neuchâtel, Rue Emile Argand 11, 2007 Neuchâtel, Switzerland

[b] Grand Rue, 04330 Barrême, France

[c] Laboratoire de Géodynamique des Chaînes Alpines, Maison des Géosciences, 38041 Grenoble Cedex, France

[d] Department of Geosciences, Geology–Palaeontology, Perolles, CH-1700 Fribourg, Switzerland

[e] UMR 8148 – I.D.E.S., Bât. 504, University of Paris XI Orsay, 91405 Orsay Cedex, France

Accepted 12 September 2005

Abstract

In the uppermost Hauterivian sediments of the western Tethys, a short-lived anoxic event (Faraoni event) is documented both in the form of an interval enriched in organic matter (pelagic realm) and in a condensed interval enriched in glauconite and phosphate (shelf realm). This latter interval represents the onset of a drowning episode on the Helvetic carbonate platform along the northern tethyan margin that lasted throughout the early Barremian. This drowning episode marks a turning point in the way the platform carbonate factory functioned: during the Hauterivian carbonate production was dominated by heterozoans, whereas during the late Barremian a photozoan assemblage developed that is preserved in the so-called Urgonian limestone. The late Hauterivian Faraoni oceanic anoxic event is of particular interest because it is not accompanied by a major positive shift in $\delta^{13}C$ unlike other oceanic anoxic events during the Cretaceous (Valanginian, early Aptian, Cenomanian–Turonian boundary).

We have analyzed four (hemi-)pelagic sections with regards to their phosphorus content to better understand the palaeoceanographic conditions related to this anoxic event and the associated changes in the shallow-water carbonate factory. The sections are located in Angles (SE France), Fiume-Bosso and Gorgo a Cerbara (central Italy), and Veveyse de Châtel-St. Denis (west Switzerland). We calculated phosphorus mass accumulation rates by using a cyclostratigraphic approach in order to obtain an adequate age model. We observe a comparable and correlatable long-term trend for the four sections, which suggests that the phosphorus mass accumulation rates and temporal changes therein are representative for the western tethyan pelagic realm. The Faraoni event is marked by a minimum in phosphorus accumulation and a positive shift in the C_{org}/P_{tot} ratios, which is interpreted as a reflection of the decreased capacity of storing and preserving phosphorus in oxygen-depleted sediments. Moreover, the onset in the decrease in phosphorus accumulation coincides with a sea level rise, while the Faraoni level itself corresponds to a maximum flooding interval. This phase of sea-level rise may have been important in the establishment of marine connections between the boreal and tethyan realms and, as such, in the exchange of nutrient-enriched waters. The model for the origin of the Faraoni oceanic anoxic event proposed here incorporates these aspects together with a positive feedback loop generated by phosphorus regeneration and a negative feedback loop related to changes in the ocean oxygen cycle.

The subsequent long-term changes in phosphorus burial rates during the Barremian suggest that the Faraoni event marks the onset of a long period of environmental instability with regards to platform growth, leading to periodic phases of eutrophication

* Corresponding author. Tel.: +41 32 718 26 05; fax: +41 32 718 26 01.
E-mail address: stephane.bodin@unine.ch (S. Bodin).

doi:10.1016/j.palaeo.2005.09.030

and drowning of the northern tethyan carbonate platform. This environmental crisis ended during the late Barremian with the onset of the deposition of the Urgonian limestone under oligotrophic conditions.

Keywords: Faraoni anoxic event; Hauterivian; Barremian; Tethys; Phosphorus accumulation rate; Platform drowning

1. Introduction

The Early Cretaceous is characterized by marked environmental and palaeoceanographic changes that are documented by episodic oceanic anoxic events, repeated platform drowning phases, and pronounced excursions in the stable carbon (C) isotope record (e.g., Lini et al., 1992; Föllmi et al., 1994; Weissert et al., 1998; Herrle, 2002). One of the less well-understood events of this period is the so-called Faraoni event (Baudin et al., 1999; Cecca et al., 1994) which is a short-lived oceanic event that occurred during the latest Hauterivian. In comparison to the other anoxic events, the Faraoni event is a rather atypical event for which the environmental circumstances are still not clear. In contrast to the anoxic events during the Valanginian, the early Aptian, and near the Cenomanian–Turonian boundary (e.g., Schlanger and Jenkyns, 1976; Schlanger et al., 1987; Weissert, 1989; Lini et al., 1992; Jones and Jenkyns, 2001; Weissert and Erba, 2004), the Faraoni level is not accompanied by a major carbon isotope excursion towards more positive values but rather by a minor long-term increase (Föllmi et al., 1994; Erba et al., 1999; Van de Schootbrugge et al., 2000). Furthermore, no major volcanic episode has, of yet, been identified for the late Hauterivian. This means that the classical model postulated for the origin of oceanic anoxic events in general, (i.e., increased volcanism leading to an increase in atmospheric CO_2, climate warming, increased weathering and nutrient availability, higher productivity and consequently higher preservation rates of organic matter (e.g., Jenkyns, 1999, 2003)) cannot be applied in this case.

The Faraoni event marks the onset of a long-lasting drowning episode on the Helvetic carbonate platform of the northern tethyan margin (D3 in Föllmi et al., 1994), which is documented by a hiatus or by the presence of condensed glauconite and phosphate-rich sediments – the so-called Altmann Beds (Funk, 1969). This drowning episode is associated with a fundamental change in the carbonate factory of this platform system. During the Hauterivian, carbonate production occurred mainly by heterozoan assemblages that are documented – for example – by the Kieselkalk Formation (Funk, 1969; Föllmi et al., 1994), whereas during the late Barremian, photozoan assemblages dominated and their debris accumulated in the widespread “Urgonian” limestone (=Schrattenkalk Formation in the Helvetic realm).

For this period and for the Early Cretaceous in general, only a limited amount of data has been obtained with regards to its phosphorus (P) record (Föllmi, 1995; 1996; van de Schootbrugge et al., 2003). P is an important and often limiting biophile element (Broecker and Peng, 1982; Ingall and Jahnke, 1994; Tyrrell, 1999) that is closely linked to the carbon (C) cycle through two interfaces: (1) biogeochemical weathering during which atmospheric CO_2 is transformed into HCO_3^- and P is mobilized; and (2) photosynthesis, which is often limited by P and by which CO_2 is transformed into organic C (e.g., Föllmi et al., 2004). A reconstruction of changes in the P cycle during this critical period may, for these reasons, help to improve our understanding of the mechanisms leading to the Faraoni anoxic event and the associated platform drowning episode.

Four pelagic or hemi-pelagic sections located in Angles (SE France), Fiume-Bosso (central Italy), Gorgo a Cerbara (central Italy) and Veveyse de Châtel-St. Denis (west Switzerland) were analyzed. By monitoring the P record in these key sections and integrating sequence–stratigraphy and cyclostratigraphy, we are able to reconstruct a general trend in P accumulation for the western Tethyan realm during the late Hauterivian and Barremian. In using the C_{org}/P_{org} and C_{org}/P_{tot} ratios, we also show that a decrease in the capacity of storing and preserving P in the sedimentary reservoir during the unfolding of the Faraoni event may have helped to sustain this anoxic event.

2. Geological setting

Four pelagic or hemi-pelagic sections in different basins within the western Tethys were selected. These sections are well dated and include the Faraoni level or its equivalent. The first studied section is the Fiume-Bosso section, located between Urbino and Gubbio, near Cagli (central Italy, Fig. 1; see also Cecca et al., 1994). It represents the type section for the Faraoni level (Cecca et al., 1994). The lithology is characteristic

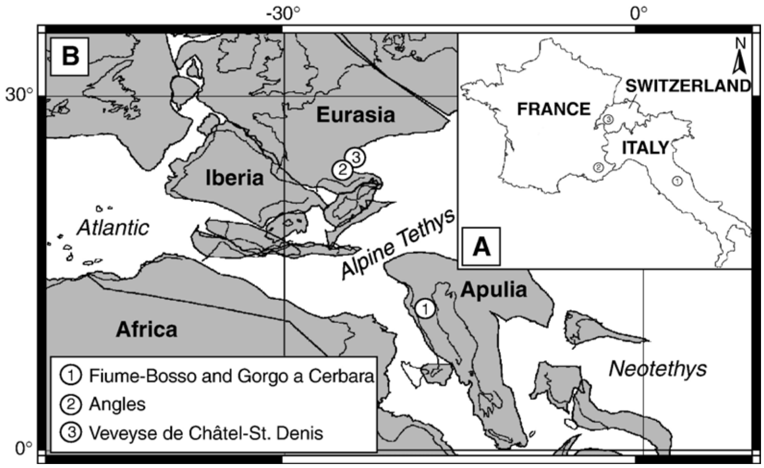

Fig. 1. (A) Localization of the four studied sections. (B) Palaeogeographic map at the Hauterivian–Barremian transition (127 Myr BP) showing the localization of the four sections (modified from Hay et al., 1999).

of the Maiolica Formation and consists of a succession of pelagic limestone beds containing abundant cherts, and locally intercalated thin organic-rich marl layers and/or laminae. The section of Gorgo a Cerbara is situated in the same area and its lithology is similar to the one of the Fiume-Bosso section. It is situated approximately 4 km east of Piobbico city along the Candigliano River (Fig. 1; see Cecca et al., 1995). This type section for the Barremian/Aptian boundary is complementary to the Fiume-Bosso section and covers the whole Barremian.

The section of the Veveyse de Châtel-St. Denis (VCD) is the third studied section. It is situated in the canton of Fribourg, along the Veveyse river, in western Switzerland (see Busnardo et al., 2003, for a detailed geographic description). Its lithology consists of a succession of alternating pelagic marl and marly limestone that are rich in macrofossils.

The fourth studied section outcrops along the "Route d'Angles", near St. André-Les-Alpes, in the Vocontian basin (S–E of France, see Busnardo (1965) for a detailed geographic description). Its lithology consists of a fossiliferous, hemi-pelagic succession of regularly alternating marl and limestone.

The palaeogeographic location of these four sections is shown in Fig. 1. During the Early Cretaceous, the Angles and the VCD sections were situated along the northern tethyan margin. The VCD section is part of the Ultrahelvetic realm, which is considered as the deeper offshore prolongation of the Vocontian basin to the northeast (Trümpy, 1960). The Fiume-Bosso and the Gorgo a Cerbara sections were located in the southern part of the tethyan realm, remote from any continent, and were surrounded by carbonate shelves. The four sections represent a N–S transect across the western Tethys.

3. Methods

3.1. Phosphorus analyses

Total phosphorus analyses were performed on bulk rock samples from the limestone intervals for all four sections. The samples were sawed in order to eliminate the altered parts and the veins of the rock. Then, powders were obtained using an agate crusher. Around 100 mg of powder were mixed with 1 ml of $MgNO_3$ and left to dry in an oven at 45 °C for 2 h. The samples were then ashed in a furnace at 550 °C during 2 h. After cooling, 10 ml of 1N HCl were added and placed under constant shaking for 14 h. The solutions were filtered with a 63-μm filter, diluted 10 times, and analyzed using the ascorbic acid method of Eaton et al. (1995). For this process, the solution was mixed with ammonium molybdate and potassium antimonyl tartrate, which, in an acid medium, reacts with orthophosphate to form phosphomolybdic acid. This acid is reduced with ascorbic acid to form an intense blue color. The intensity of the blue color is determined with a photospectrometer (Perkin Elmer UV/Vis Photospectrometer Lambda 10). The concentration of PO_4 in mg/l is obtained by calibration with known standard solutions. Individual samples were measured three times and precision was better than 5%. Replicate analyses of samples have a precision better than 10% in the case of low P concentration (such as in samples of the Fiume-Bosso and Gorgo a Cerbara sections) and better than 7% in the two other sections.

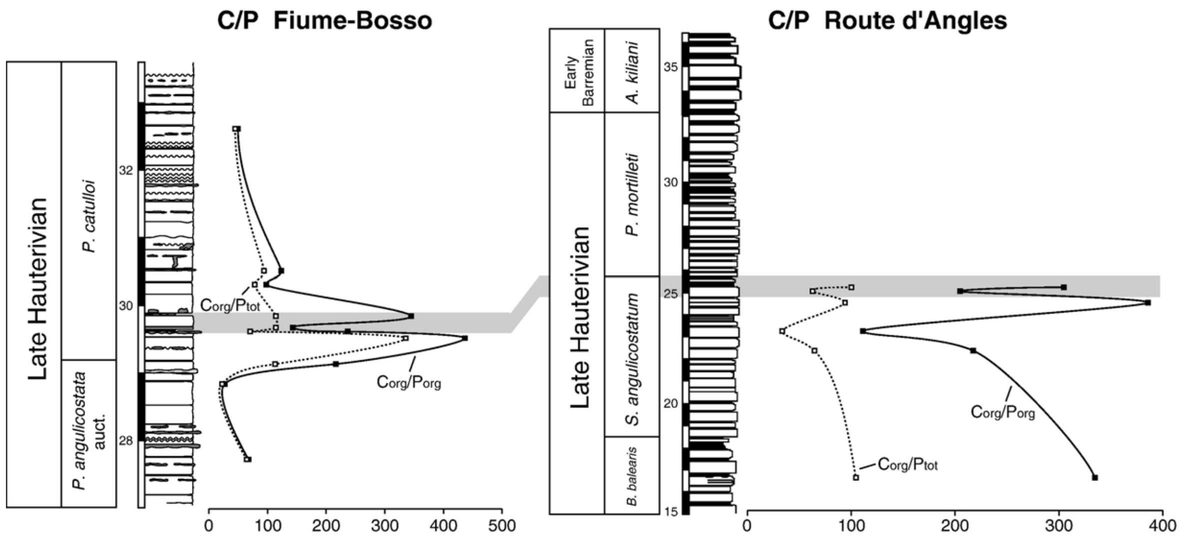

Fig. 2. C/P_{org} and C/P_{tot} ratios (expressed in mol/mol) in the Fiume-Bosso and Angles sections. The grey band traces the Faraoni level.

Total P content in marls was determined using the same method as for the limestone. P content of the organic matter was determined by using a sequential extraction technique adapted from the SEDEX method developed by Ruttenberg (1992) and modified by Anderson and Delaney (2000). As for total phosphorus, the solutions were diluted ten times, colored using the ascorbic acid method of Eaton et al. (1995) and analyzed with a photospectrometer (Perkin Elmer UV/Vis Photospectrometer Lambda 10).

Table 1
TOC (%), P_{org} (ppm), P_{tot} (ppm) and calculated C/P_{org} and C/P_{tot} ratios for the marls samples of the Fiume-Bosso, Angles and VCD sections around the Faraoni level

Ech	TOC (%)	[P_{org}] (ppm)	[P_{tot}] (ppm)	C_{org} (mmol/g)	P_{org} (mmol/g)	P_{tot} (mmol/g)	C_{org}/P_{org}	C_{org}/P_{tot}
Fiume-Bosso								
FB 133	2.11	786.7	809.0	1.760	0.0254	0.0261	69.3	67.4
FB 138	1.12	1001.1	1280.0	0.931	0.0323	0.0413	28.8	22.5
FB 372	4.51	540.5	1011.0	3.752	0.0174	0.0327	215.0	114.9
FB 374	14.81	871.0	1130.2	12.329	0.0281	0.0365	438.5	337.9
FB 377	1.12	120.8	404.4	0.931	0.0039	0.0131	238.6	71.3
FB 379	4.99	897.6	1091.0	4.152	0.0290	0.0352	143.3	117.9
FB 381b	3.65	274.3	813.8	3.037	0.0089	0.0263	343.0	115.6
FB 384	3.69	954.8	1195.6	3.073	0.0308	0.0386	99.7	79.6
FB 386	4.25	902.6	1163.7	3.537	0.0291	0.0376	121.4	94.2
FB 397	2.02	1014.7	1094.5	1.679	0.0328	0.0353	51.3	47.5
Angles								
AN32b	2.63	202.8	668.7	2.191	0.0065	0.0216	334.6	101.5
AN46b	2.13	251.3	894.1	1.769	0.0081	0.0289	218.1	61.3
AN48b	1.11	256.9	942.4	0.926	0.0083	0.0304	111.6	30.4
AN51b	1.09	72.8	311.6	0.908	0.0024	0.0101	386.3	90.3
AN52b	1.49	186.5	645.2	1.244	0.0060	0.0208	206.6	59.7
AN53.1b	1.09	92.0	289.7	0.906	0.0030	0.0094	304.9	96.9
Veveyse								
VCDII 11B	0.37	127.2	263.0	0.305	0.0041	0.0085	74.2	35.9
VCDII 14B	0.31	103.5	258.4	0.258	0.0033	0.0083	77.2	30.9
VCDII 17B	0.73	154.4	380.4	0.604	0.0050	0.0123	121.1	49.2
VCDII 18B	0.61	159.2	410.4	0.505	0.0051	0.0132	98.3	38.1
VCDII 20B	0.78	146.0	315.3	0.645	0.0047	0.0102	137.0	63.4

Table 2
Calculated duration of the different ammonite or magnetochron zones within the four sections

Angles

Ammonite zone	20 kyr bundles	Duration
B. balearis (at least)	35	700 000
S. angulicostatum	21	420 000
P. mortilleti	24	480 000
A. kiliani	25	500 000
K. nicklesi	20	400 000
N. pulchella	20	400 000
K. compressissima	20	400 000
C. darsi	17	340 000
H. uhligi	12	240 000
H. sayni	28	560 000
G. sartousiana	20	400 000
H. feraudianus	23	460 000
I. giraudi	16	320 000
M. sarasini	25	500 000
D. oglanlensis (at least)	20	400 000
Late Hauterivian (at least)	80	1 600 000
Lower Barremian	102	2 040 000
Upper Barremian	124	2 480 000
Lowermost Aptian (at least)	20	400 000
Barremian	226	4 520 000
Beginning of Faraoni level to H/B boundary	25	500 000

Fiume-Bosso

Ammonite zone	100 kyr bundles	Duration
B. balearis (at least)	8	800 000
P. angulicostata auct.	8	800 000
P. catulloi (subzone)	5.5	550 000
S. hugii (at least)	3	300 000
Beginning of Faraoni level to H/B boundary	5	500 000

Veveyse de Châtel-St. Denis

Ammonite zone	20 kyr bundles	Duration
S. sayni (at least)	34	680 000
P. ligatus	25	500 000
B. balearis	36	720 000
P. angulicostata auct.	52	1 040 000
T. hugii (at least)	12	240 000
Beginning of Faraoni level to H/B boundary	21	420 000

Gorgo a Cerbara

Magnetochron	100 kyr bundles	Duration
M-4 (at least)	6	600 000
M-3	17.5	1 750 000
M-2	6	600 000
M-1	3.5	350 000
M-1n	22	2 200 000
M-0	3.3	330 000
Late Hauterivian (at least)	5	500 000
Lower Barremian	16	1 600 000

Table 2 (*continued*)

Gorgo a Cerbara

Ammonite zone	20 kyr bundles	Duration
Upper Barremian	33.3	3 330 000
Lowermost Aptian (at least)	4	400 000
Barremian	49.3	4 930 000
Beginning of Faraoni level to H/B boundary	5	500 000

The values obtained for the first and the last ammonite zone or magnetochron for each section is a minimum value.

C_{org}/P_{org} and C_{org}/P_{tot} ratios were determined in the marls within and around the Faraoni level for three sections (Fiume-Bosso, Angles and VCD). The C concentration was obtained by Rock-Eval pyrolysis (Behar et al., 2001) using the standard temperature cycle. Two standards (an in-house standard and the "IFP 160000" standard from the Institut Français du Pétrole, Paris, France) were analyzed at the beginning and at the end of a batch of ca. 15 samples. C/P is expressed in mol/mol unit (Fig. 2). The results for TOC and phosphorus are shown in Table 1.

3.2. Age model

In order to avoid problems of condensation and to better compare the different sections, we decided to calculate phosphorus accumulation rates (PAR). The PAR is expressed in mg of P per cm^2 per kyr. This is a multiplication of the concentration in P (mg/g), the density (g/cm^3), and the sedimentation rate (cm/kyr). As all the samples are pelagic or hemi-pelagic mudstones, the density was assumed to be constant and equal to 2.5 g/cm^3 for all analyzed samples.

An age model was obtained for the four sections by a cyclostratigraphic approach (Table 2). For the Angles section, following the study of Giraud et al. (1995) in the late Hauterivian (*angulicostata* zone) sediment of Vergons, we considered that each limestone–marl couplet represents a duration of 20 kyr. We estimated such an average sedimentation rate for the successions of sediments that correspond to the time envelopes of complete ammonite zones (Vermeulen, 2002). It appears that in the Angles section, the *sartousiana* and the *feraudianus* zones are not complete due to the presence of hiatuses and/or condensed sediments (Delanoy, 1997; Vermeulen, 2002; see also Wissler et al., 2002). For the sediments attributed to these two ammonite zones, we decided to use the time envelopes for the corresponding sedimentary intervals from the Saut-du-Loup section, which is situated in the same area (close to Barrême) and appears to be more complete (Vermeulen, 1980). For the Fiume-Bosso and the Gorgo a Cerbara sections, we followed the method described in Fiet and Gorin (2000) to discriminate 100-kyr bundles in Barremian carbonate-dominated pelagic deposits of central Italy, and then determine sedimentation rates based on the eccentricity bundles.

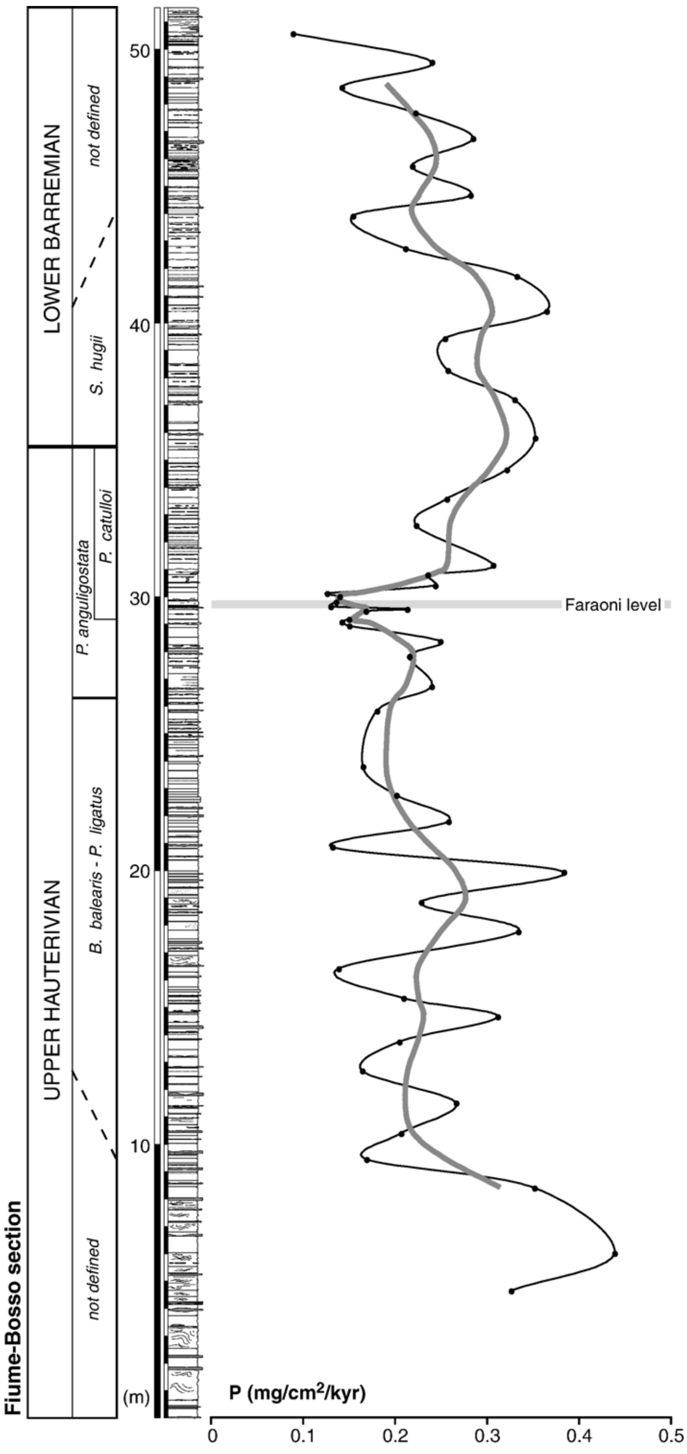

Fig. 3. Fiume-Bosso PAR values. The trend curve is calculated using a five point moving average formula. Biostratigraphy after Coccioni et al. (1998).

Finally, in the VCD section, the same method as for the Angles section was applied. The ammonite zones have been defined by Busnardo et al. (2003), and their limits are dated approximately by Hardenbol et al. (1998). By counting the limestone–marl alternations between these limits, an average time span of 20 kyr is suggested for one limestone–marls couplet. Occasionally it is observed that five couplets group into bundles, which would then correspond to 100 kyr. These frequencies imply that sedimentation was controlled by orbital cycles in the Milankovitch frequency band.

We find a duration of 500 kyr for the interval between the base/onset of the Faraoni level and the Hauterivian–Barremian boundary in three sections (Fiume-Bosso, Gorgo a Cerbara and Angles). In the VCD section, the calculated duration is equal to 420 kyr. This slight difference reflects the limits of the cyclostratigraphy approach. In the Angles section, the duration of the Barremian is estimated to be equal to 4.52 Myr (with the integration of the duration of the *sartousiana* and *feraudianus* zones from the Saut-du-Loup section). This duration is in relatively good agreement with those obtained by Fiet and Gorin (2000) for the Barremian of the Gorgo a Cerbara section (5.11 ± 0.34 Myr) and the estimate of the age of the Barremian proposed by Gradstein et al. (2004) (between 130 ± 1.5 and 125 ± 1.0 Myr BP). However, a discrepancy exists with the study of Wissler et al. (2004), who found a duration of 4 Myr between the top of Chron M3 and the base of Chron M0, which is not in good agreement with our estimate of 3.15 Myr for the same time interval at Gorgo a Cerbara.

4. Results

4.1. The Fiume-Bosso section

The PAR values vary between 0.09 and 0.44 mg/cm^2/kyr (Fig. 3). In the lower part of the section (below the *angulicostatum* auctorum zone), the long-term trend appears more or less constant (approximately 0.21 mg/cm^2/kyr) despite high-frequency fluctuations. Then, within the *angulicostatum* auctorum zone, the values begin to decrease and reach a minimum (0.13 mg/cm^2/kyr) around the Faraoni level. Above the Faraoni level, the values increase and reach a maximum in the sediments approximately 10 m above the Faraoni level. In the upper part of the section, we observe again a decrease in the PAR trend.

The C_{org}/P_{org} ratios measured in marly intervals within and around the Faraoni level show two closely spaced excursions toward values between 300 and 450 near and within the Faraoni level, whereas background values vary between 50 and 100 (Fig. 2). The C_{org}/P_{tot} ratios show approximately the same behaviour as the C_{org}/P_{org} ratios but with lower absolute values. Near or within the Faraoni level, values are higher than 114 (with the exception of one sample), whereas the other samples have values between 20 and 100.

4.2. The Veveyse de Châtel-St. Denis section

The VCD section displays the highest PAR values of this work (Fig. 4). They vary between 0.98 and 3.48 mg/cm^2/kyr, with a mean value of 1.82 mg/cm^2/kyr. In the lower part of the section (*sayni* zone), a decrease in PAR is first observed, with values reaching a minimum at the *sayni–ligatus* boundary. A strong increase follows and PAR values reach a maximum within the *balearis* zone. The sediments attributed to the late *balearis*–early *angulicostata auct*. zones are marked by generally low PAR values and a decreasing trend. A short positive shift is distinguished in the middle of the *angulicostata auct.* zone. We note that the sediments considered to represent the equivalent of the Faraoni level are marked by a negative shift in PAR. Finally, the upper part of the section shows an increase in PAR values.

The C/P ratios are very low, with an average value close to 100 for the C_{org}/P_{org} ratios and close to 45 for the C_{org}/P_{tot} ratios. No specific trend is distinguished.

4.3. The Angles section

The sediment succession of the Angles section studied here represents the time interval between the *balearis* zone (late Hauterivian) and the *oglanlensis* zone (earliest Aptian). This specific section yielded the most variable PAR curve (Fig. 5). PAR values vary between 0.57 and 1.96 mg/cm^2/kyr, with an average value of 1.08 mg/cm^2/kyr. After a more or less constant trend in sediments attributed to the *balearis* zone (mean value of 1.28 mg/cm^2/kyr), an initial decrease is observed in sediments of the *angulicostatum* zone (Vermeulen, 2002), and a minimum in PAR values is reached within the Faraoni level (0.57 mg/cm^2/kyr). Higher up in the section, the trend in PAR values increases again up to the sediments of the latest *nicklesi* zone. A small positive shift is observed in sediments of the middle *kiliani* zone. In sediments from the *pulchella* to the *darsi* zones, the values are firstly rapidly decreasing and then become more or less constant with a positive shift in sediments dating from the beginning of the *compressissima* zone. Subsequently, the PAR

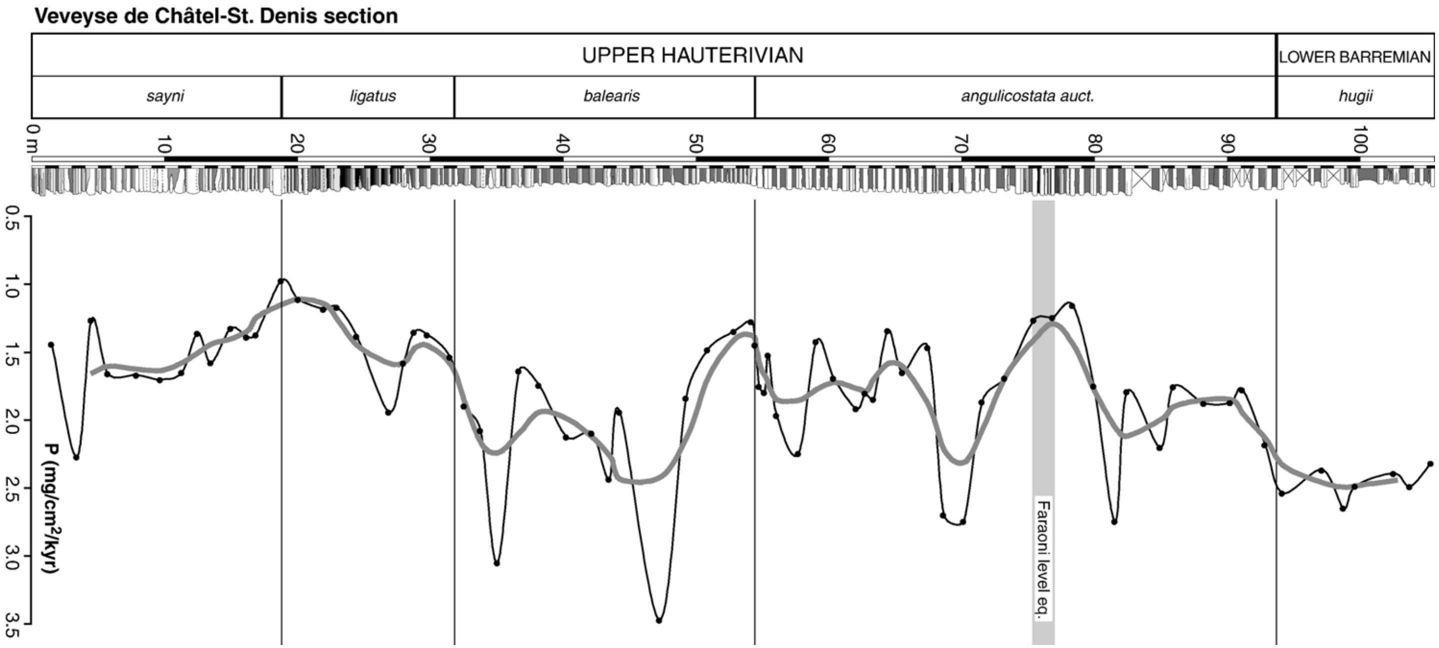

Fig. 4. Veveyse PAR values. The trend curve is calculated using a five point moving average formula. Biostratigraphy modified after Busnardo et al. (2003).

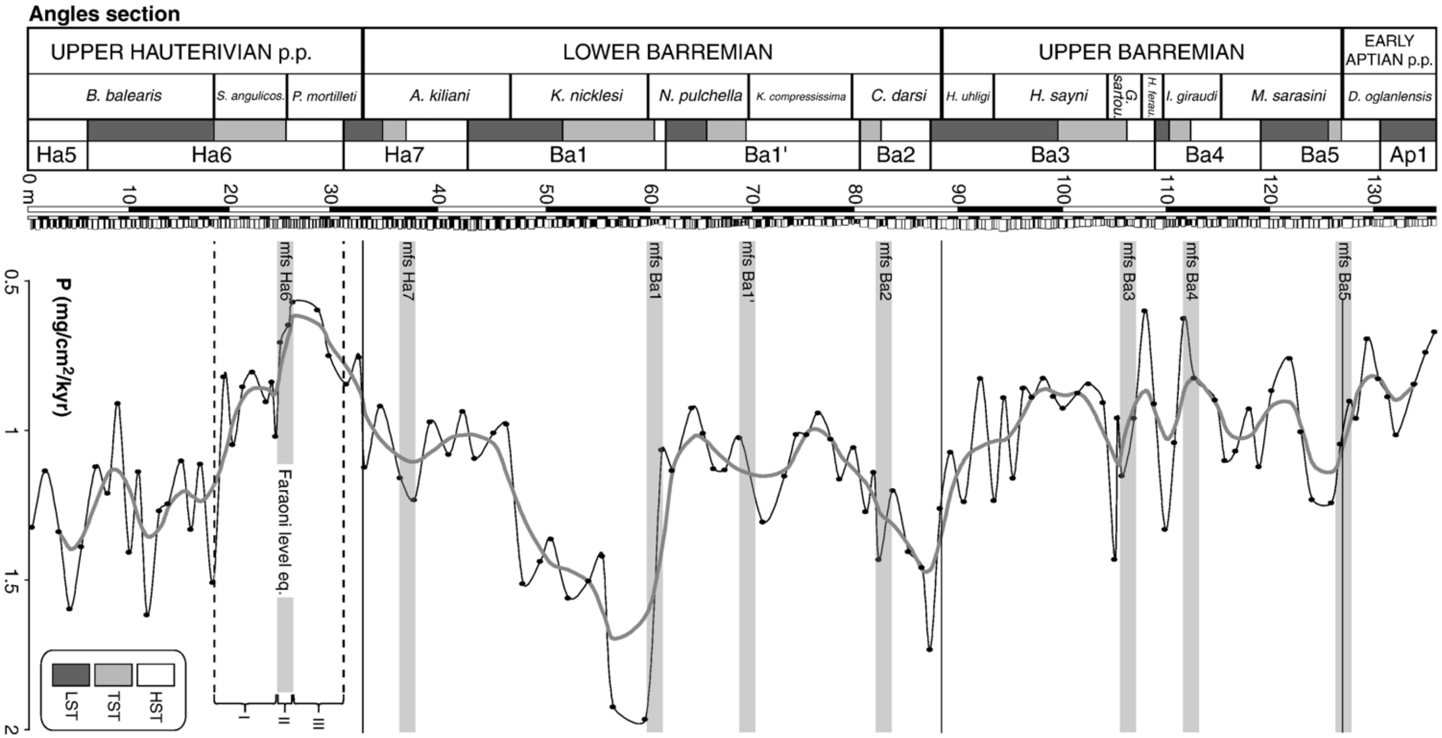

Fig. 5. Angles PAR values. The trend curve is calculated using a five point moving average formula. Biostratigraphy after Vermeulen (2002). I, II and III refer to the model stages developed in Fig. 7.

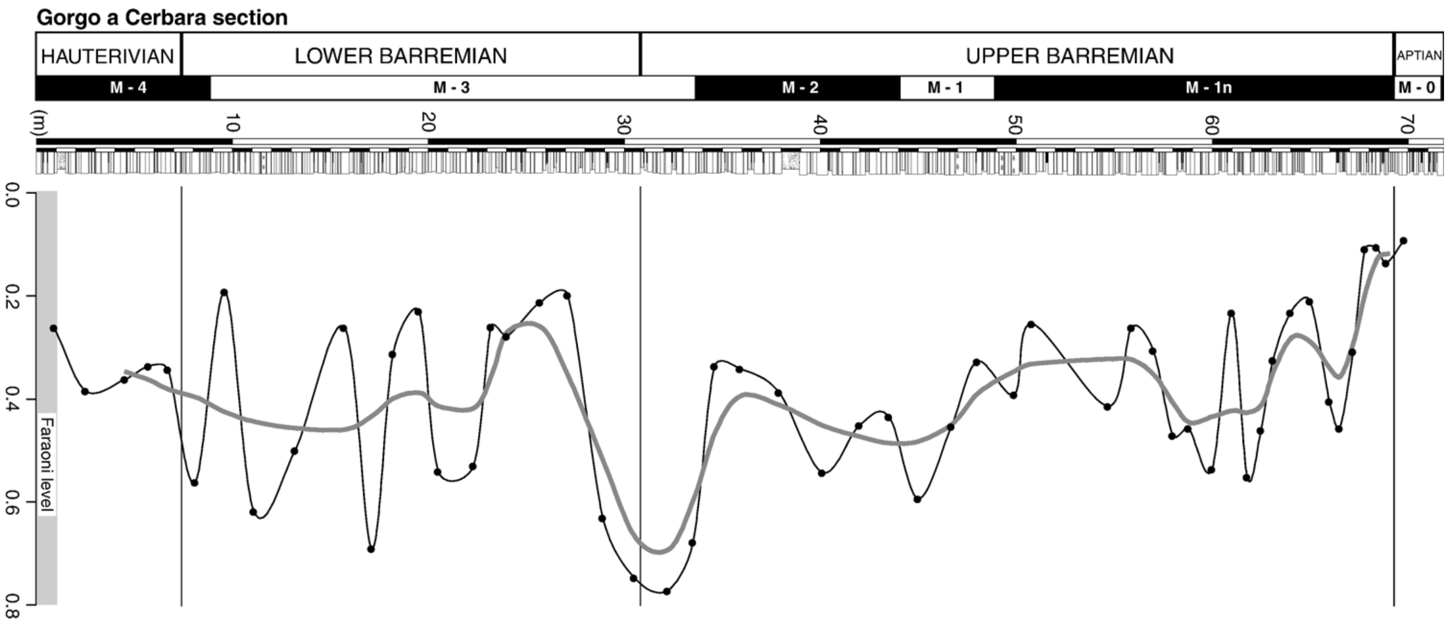

Fig. 6. Gorgo a Cerbara PAR values. The trend curve is calculated using a five-point moving average formula. Modified after Fiet and Gorin (2000).

values are increasing up to the end of the *darsi* zone. Finally, in the sediments near the top of the section dated as late Barremian–earliest Aptian, the long-term trend appears more or less constant (around 0.98 mg/cm^2/kyr) despite some high-frequency fluctuations (especially in sediments of the *sartousiana–feraudianus* zones).

The C_{org}/P_{org} ratios are clearly enriched around the Faraoni level (with a twofold peak and a maximum value of 386). Approximately 8 m below the Faraoni level, a second peak near 330 is distinguished (Fig. 2). The same behaviour is seen for the C_{org}/P_{tot} ratios, but with a maximum value of 102 for the enriched samples.

4.4. The Gorgo a Cerbara section

The PAR values vary between 0.08 and 0.77 mg/cm^2/kyr (Fig. 6). Sediments belonging to the early Barremian and the early–late Barremian boundary transition are characterized by two strong positive shifts (the values exceed 0.60 mg/cm^2/kyr in both shifts). In sediments attributed to the late Barremian, a slightly diminishing trend of around 0.30 mg/cm^2/kyr is distinguished, along with higher frequency fluctuations.

5. Discussion

5.1. Phosphorus accumulation

The flux of dissolved, bioavailable P into the ocean is mainly controlled by continental runoff and atmospheric transport (Föllmi, 1996; Delaney, 1998; Benitez-Nelson, 2000; Compton et al., 2000). The removal of bioavailable P from the ocean reservoir is given by the difference between the rate of P sedimentation and its return flux from the sedimentary reservoir. The transfer of bioavailable P into the sedimentary reservoir occurs either by sedimentation of organic matter bound P, P adsorbed on clay particles and Fe- and Mn-oxyhydroxides, P in fish debris, or by direct (microbial?) precipitation of dissolved inorganic P (e.g., Ruttenberg, 1993; Filippelli and Delaney, 1996; Föllmi, 1996). Early diagenetic regeneration of P and its removal from the sediments is an important process (Broecker and Peng, 1982; Colman and Holland, 2000; Tamburini et al., 2002, 2003; but see also Anderson et al., 2001). The efficiency of P storage in the sedimentary reservoir is redox dependent, and P regeneration becomes more important in oxygen-depleted bottom waters (Ingall and Jahnke, 1994; Van Cappellen and Ingall, 1996; Colman and Holland, 2000; Emeis et al., 2000). The redox-sensitive capacity of P storage in the sedimentary reservoir may result in a positive feedback mechanism between water-column anoxia, enhanced benthic phosphorus regeneration, and increased marine productivity (Ingall and Jahnke, 1994, 1997; Van Cappellen and Ingall, 1996; Colman and Holland, 2000).

The rate of P accumulation integrated over larger areas and time scales exceeding the actual residence time of P (approximately 10 kyr; Ruttenberg, 1993; Filippelli and Delaney, 1996; Colman and Holland, 2000) is therefore driven by two main processes: (1) the combined river and atmospheric input of P, which is linked to the rates of continental weathering, erosion, and runoff; and (2) the degree of bottom-water oxygenation. As such, an increase in PAR indicates either an increase in the intensity of continental weathering and erosion rate, for example, induced by a more humid climate and/or an increase in bottom-water oxygenation. On the other hand, a decrease in PAR indicates either a decrease in continental weathering rates, related for example to a change to a drier climate, or a spread of dysaerobic to anoxic bottom-waters, or the combined effect of both processes.

5.2. The C/P molar ratio

In the Fiume-Bosso and Angles sections, the marls associated with the Faraoni level are marked by an increase of the C_{org}/P_{org} molar ratio in preserved organic matter to maximal values of 400. The marls in and around the equivalent of the Faraoni level of the VCD section yielded very low TOC values (<0.5%), and an interpretable C/P molar ratio could not be obtained. The measured C_{org}/P_{org} molar ratios deviate from the Redfield ratio (106:1; Redfield, 1958), which implies that the preserved organic matter is depleted in phosphorus relative to carbon. Ingall et al. (1993), Ingall and Jahnke (1994, 1997), Van Cappellen and Ingall (1996), and Slomp et al. (2004) associated increased C_{org}/P_{org} molar ratios in organic matter with the degradation of organic matter and the relative loss of organic phosphorus under the influence of water column anoxia, which would concur with the overall minimal values in P accumulation rates during the Faraoni anoxic event. Interestingly, a twofold spike in C_{org}/P_{org} molar ratio is present in both sections, which may suggest that the unfolding of anoxic conditions may not have been uniform, but stepwise, with an intermittent return to more normal conditions. Within the Faraoni level, the C_{org}/P_{tot} molar ratio appears to trace well the lower spike in the twofold spike in the C_{org}/P_{org} ratio; the upper spike is less markedly traced.

Following Anderson et al. (2001), it appears that the $C_{org}/P_{reactive}$ molar ratio ($P_{reactive} = P_{oxide\text{-}associated} + P_{authigenic} + P_{org}$) is a more robust measure of the degree of P lost to the ocean than C_{org}/P_{org} molar ratio, due to the possible diagenetic transfer of organic phosphorus into an authigenic phase. In ancient marine sedimentary rocks, the chemical distinction between the $P_{authigenic}$ and $P_{detritic}$ phases is, however, difficult (e.g., Filippelli and Delaney, 1995), and we decided, therefore, to analyze P_{tot} and to calculate the C_{org}/P_{tot} ratio ($P_{tot} = P_{reactive} + P_{detritic}$). Silt- and sand-sized detrital material is quasi absent in the here analyzed (hemi-)pelagic sections, and the presence of detrital phosphate seems minimal but cannot be totally excluded. The here presented C_{org}/P_{tot} ratio is therefore a minimal value, and the ratio approaching the effective quantity of organic phosphorus that was transferred into an authigenic phase and remained as such within the marly bed lies somewhere between the C_{org}/P_{tot} and C_{org}/P_{org} molar ratios.

At Fiume-Bosso, pre- and post-Faraoni sediments show C_{org}/P_{tot} and C_{org}/P_{org} molar ratios that are almost identical and mostly substantial lower than the Redfield ratio, whereas the organic-rich Faraoni sediments have higher C_{org}/P_{tot} and C_{org}/P_{org} molar ratios. The low and almost identical pre- and post-Faraoni C_{org}/P_{tot} and C_{org}/P_{org} molar ratios suggest that practically all P is conserved as P_{org} and that the organic matter is depleted in C_{org} relative to P_{org}, most likely by bacterial degradation (e.g., Reimers et al., 1990). The Faraoni sediments show systematically lower C_{org}/P_{tot} than C_{org}/P_{org} ratios that are all slightly to markedly higher than the Redfield ratio, with the exception of one sample (Fig. 2). This pattern suggests that during early diagenesis of the organic-rich sediments of the Faraoni level, P_{org} was preferentially mobilized (relative to C_{org}) and a transfer of P_{org} took place both into an authigenic phase as well as out of the organic-rich layer, most likely back into the bottom water. This systematic stratigraphic change in C_{org}/P_{tot} and C_{org}/P_{org} molar ratios in and around the Faraoni sediments suggests that under normal conditions, a preferential loss of C_{org} relative to P_{org} took place, whereas under the more anoxic conditions during the deposition of the Faraoni level, a preferential loss of P_{org} relative to C_{org} is observed that is related both to a transfer of P_{org} into an authigenic phase as well as out of the initial layer back into the seawater.

For the Angles section, the C_{org}/P_{tot} molar ratios are systematically lower than the C_{org}/P_{org} molar ratios, both within the sediments of the Faraoni equivalent, as well as around this level. This pattern may indicate that in all the analyzed marl samples, P_{tot} is a composite of P_{org} and $P_{authigenic+detritic}$. The C_{org}/P_{org} molar ratios are all higher than the Redfield ratio, whereas the C_{org}/P_{tot} molar ratios are lower or near the Redfield ratio. This may signify that a systematic transfer took place of P_{org} into an authigenic P phase, whereas – in contrast to the Fiume-Bosso section – a diagenetic transfer of P back to the seawater is less likely. In addition, due to the paleogeographic position of Angles close to the European continent, a more significant influx of $P_{detritic}$ than at Fiume-Bosso cannot be excluded. Moreover, in the Angles section, TOC values are generally low (mean value close to 1.5%), and the Faraoni level is not as much enriched as could be expected from a basinal record (cf. Fiume-Bosso results, Table 1). This may hint at the possibility of late-stage diagenetic alteration of organic matter coupled with the preferential loss of C_{org}. These two mechanisms could thus also be responsible of the negative shift of the Angles C_{org}/P_{tot} molar ratios relative to the C_{org}/P_{org} molar ratios.

5.3. Comparison of the PAR curves between the four sections

The PAR of the Fiume-Bosso and the Gorgo a Cerbara sections are characterized by low average values whereas the VCD section shows PAR values that are about eight times higher than those of the Fiume-Bosso and Gorgo a Cerbara sections. This difference in absolute PAR values is likely related to the different paleogeographic positions of the sections. The paleogeographical location of the Fiume-Bosso and Gorgo a Cerbara sections is remote from any continental source, and the low PAR, which are comparable to the PAR values from the ODP and DSPD compilation from Föllmi (1995), indicate generally low detrital influx rates. Moreover, the values of the VCD section, which are high also compared to those of the Angles section, indicate that along the northwestern tethyan margin the Ultrahelvetic realm received more detrital material than the Vocontian Basin during the time period studied. In the field, the more marly facies of the Ultrahelvetic carbonates supports this observation.

The good overall correlation between the PAR trend calculated for the four sections, as well as with the PAR trend given by Föllmi (1995) and van de Schootbrugge et al. (2003), suggests that the evolution in PAR during the late Hauterivian and the Barremian is similar over wide areas within the western Tethys (Fig. 7). PAR values show a first minimum close to the *sayni–ligatus* zone boundary, which was

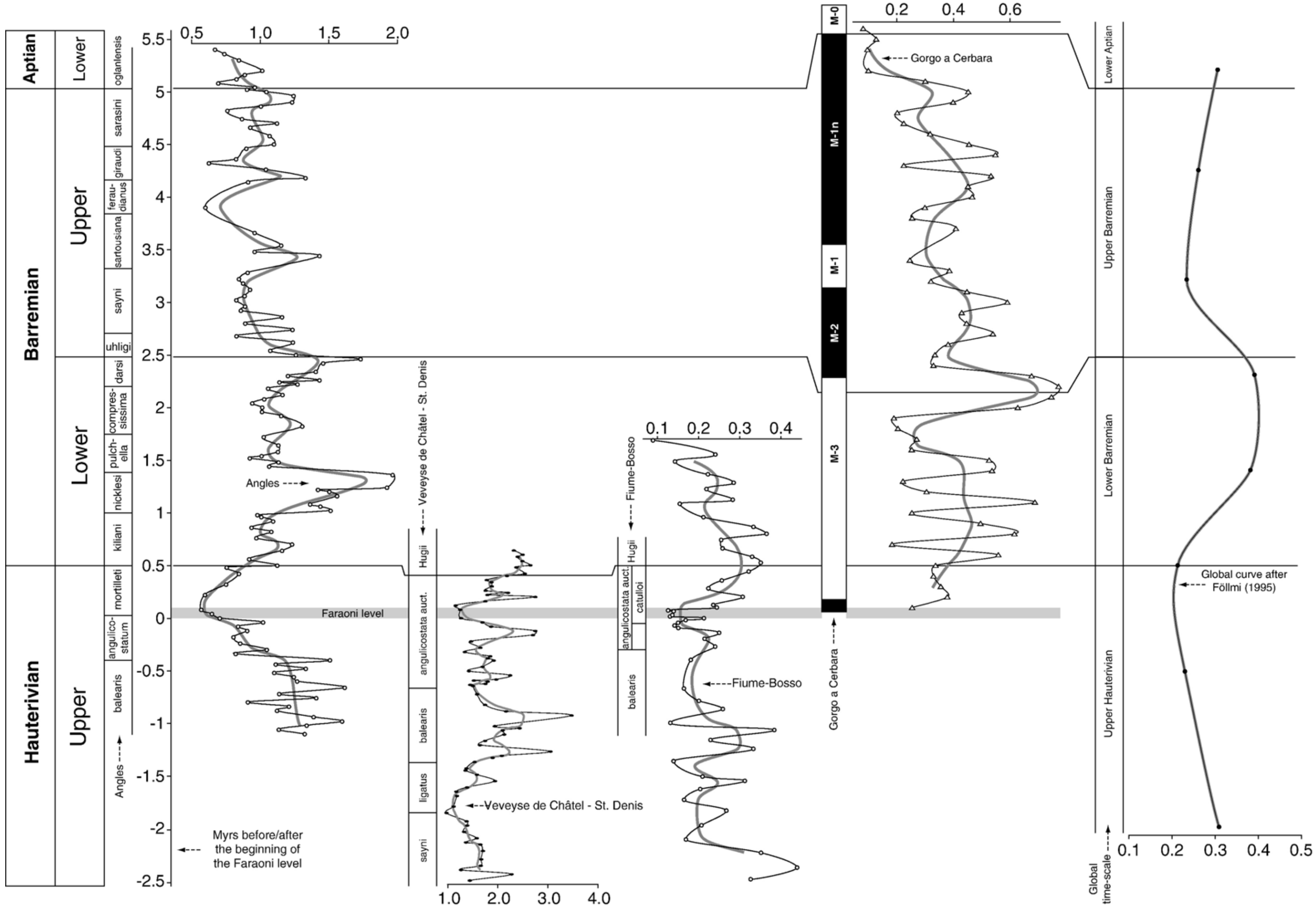

Fig. 7. Correlation of the PAR values from the four studied sections and the global curve established by Föllmi (1995). The absolute PAR values being different for the four sections, the curves are not to scale to better compare the different variations of the PAR values. The absolute ages, in regard to the beginning of the Faraoni level, were obtained using cyclo-stratigraphic interpretations (see text for explanation).

already described by van de Schootbrugge et al. (2003) for the Tethyan realm. In the absence of known anoxia events during this time, this may be explained by low nutrient influx rates into the Tethyan realm during the early late Hauterivian. PAR values show subsequently a general increase until the *balearis* zone, which is followed by a general decrease towards the Faraoni level. In the Fiume-Bosso, Angles and VCD sections, the Faraoni level itself is marked by a minimum in PAR values. In sediments above the Faraoni level, PAR values increase again in all four sections. The early Barremian is thus characterized by relatively high values in the four studied sections as well as in the global curve of Föllmi (1995). Following Bréhéret (1994) and Erba et al. (1999), the early Barremian in the western tethyan realm is characterized by the deposition of black shales that appear contemporaneous with the positive peaks in PAR. Finally, in the late Barremian, PAR values are more or less constant (with a slight decrease), although the global curve of Föllmi (1995) shows a slight increase (Fig. 7). In the Italian sections, extreme fluctuations are observed during the late Hauterivian and the early Barremian. Moreover, in these sections, many thin and isolated black-shale horizons are found during this time interval, arguing for local and short-lived anoxic conditions during the late Hauterivian–early Barremian within the Umbria-Marche basin.

5.4. The Faraoni oceanic anoxic event

The latest Hauterivian minimum in PAR values observed in the Fiume-Bosso, Angles and VCD sections coincides with the Faraoni level, which may hint at a causal relationship between late Hauterivian PAR behaviour and the Faraoni anoxic event. If this is the case, then the decrease in PAR values during the late Hauterivian may well be the consequence of a progressive loss of oxygen in oceanic bottom waters, with the Faraoni anoxic event as a result of the culminating effect of the loss of oxygen that may have started in the late *balearis* zone. This could also explain the presence of the pronounced negative shift in the VCD section during the *angulicostata auct.* zone below the Faraoni level. Eventual anoxic conditions may have developed earlier than in shallower regions, which were bathed in oxygen-depleted bottom waters only later, due, for example, to the progressive vertical expansion of an oxygen minimum zone. The minimum in PAR is probably related to a general decrease both in the capacity of transferring P into the sedimentary reservoir as well as in the capacity of preserving P within the sedimentary reservoir, as is indicated by the C/P molar ratios in Fiume-Bosso – both dependent on oxygen contents in the bottom waters.

For the Angles section, a detailed study of the trends in stacking patterns has been made that was used for a sequence–stratigraphic interpretation (Fig. 5). This allows us to compare the PAR curve with the inferred sequence–stratigraphic trends. It appears that almost every maximum in PAR values is related to a maximum flooding surface (mfs), except for of the Faraoni level and the mfs Ba4, which are characterized by a minimum in PAR values. Interestingly, the sea-level lowstands are not characterized by high PAR values. These observations correlate well with the observations of Föllmi (1995) who noted a positive correlation between sea level and phosphorus burial during greenhouse climates. A clear difference in the nutrient cycle between greenhouse and icehouse conditions is thus underlined in the Barremian sediments of the Angles section. Below the Faraoni level, the onset of the PAR decrease coincides with the transgressive surface (ts) of Ha6 and the minimum in PAR values with the mfs Ha6.

This relation suggests the presence of a link between the Faraoni anoxic event and the late Hauterivian phase of sea-level rise (Ha6), which represent an important transgression during the late Hauterivian and early Barremian (Haq et al., 1987; Hardenbol et al., 1998). During this transgression, straits connecting the tethyan and boreal realms were opened and/or became broader and deeper, as is suggested by belemnite migration patterns observed by Mutterlose and Bornemann (2000) and the presence of boreal nannoplankton in the Angles section around the Faraoni level (Silvia Gardin, personal communication). This bathymetric change may have led to the increased influx of colder and eventually more nutrient-rich waters into the Tethys, as was also proposed for the middle Hauterivian transgression (van de Schootbrugge et al., 2003).

During greenhouse conditions, a link between sea-level change and nutrient influx has been noted by different authors (e.g., Jenkyns et al., 1994; Föllmi, 1995; Hilbrecht et al., 1996; Gale et al., 2000; Jarvis et al., 2002; van de Schootbrugge et al., 2003), and different mechanisms have been proposed:

(1) Jarvis et al. (2002) invoked reworking of sediments and soils by flooding of land areas to explain the increase in nutrient fluxes during transgression. The peculiar palaeogeography of

the Cretaceous world, characterized by the presence of extensive shallow epicontinental seas during high sea level, may have favoured this process.

(2) An additional mechanism may have been provided by intensified sea surface-water evaporation due to the enhanced surface of epicontinental seas: intensified evaporation may have lead to increased wind velocities (e.g., Iruthayaraj and Morachan, 1978), which may have resulted in stronger coastal upwelling and in increased availability of nutrients during sea-level rise.

(3) A third mechanism that relates sea-level with nutrient supply is climate: transgression, climate warming, and enhanced evaporation may accelerate the global water cycle and intensify precipitation on the continent, which again favours biogeochemical weathering and the release of biophile elements (e.g., Föllmi, 1996).

(4) A positive feedback between water-column anoxia, enhanced benthic phosphorus regeneration, and marine productivity during transgressions should also be taken into account (Ingall and Jahnke, 1994, 1997). This mechanism, however, appears to be balanced by the phosphorus–oxygen negative feedback loop described by Holland (1994) and Lenton and Watson (2000). In this model, the amount of phosphorus dissolved in the water is influenced by changes in the levels of dissolved oxygen in the water column. The decrease of the burial of organic and iron-bound phosphorus under oxygen-depleted conditions in ocean bottom waters tends to increase the ocean nutrient inventory and provide negative feedback against declining oxygen by increasing the population of oxygen-producing organisms.

In taking into account the observed link between the minima in the PAR record accompanying the oceanic anoxic Faraoni event, we propose the following model (Fig. 8):

(1) The third-order sea-level rise during the late Hauterivian (Ha6 transgression: Haq et al., 1987; Hardenbol et al., 1998) led to a combination of the above-mentioned mechanisms (i.e., reworking of sediments and soils on flooded land areas, stronger evaporation rates, stronger winds and stronger upwelling, stronger biogeochemical weathering), which – together with enhanced tethyan–boreal connection and the influx of colder and eventually nutrient-rich waters – resulted in increased nutrient input into the Tethys. The resulting increase in primary productivity and corresponding export production induced a decrease in oceanic oxygen levels and the expansion of the oxygen minimum zone. The spreading of oxygen-depleted ocean bottom waters may have resulted in enhanced P regeneration from the sediments that also contributed to a further fertilisation of the ocean. During this time interval, true anoxic conditions were not reached on a global scale, and short-lived anoxic conditions were only locally present. During the late Hauterivian sea-level rise, the phosphorus–oxygen negative feedback loop described by Holland (1994) and Lenton and Watson (2000) may have been overwhelmed by the coupled positive feedback mechanism leading to higher nutrient concentrations, and may have been too weak to balance the decrease in oceanic oxygen levels.

(2) During the period of most rapid sea-level rise (mfs Ha6), these coupled mechanisms reached their climax and resulted in the Faraoni oceanic anoxic event. This event may be considered as the result of a steady-state situation in which the positive feedback mechanisms leading to increased nutrient availability are balanced by the negative feedback mechanisms (phosphorus–oxygen negative feedback coupled with organic matter preservation). The limestone–black shale alternation that is characteristic of the Faraoni level in the four investigated sections and elsewhere may then be explained by high-frequency oscillations superimposed on this steady-state situation.

(3) During subsequent sea-level highstand (highstand systems track of Ha6), the rapid filling of shallow-water areas by sediments may have diminished the importance of the tethyan–boreal connection and the associated nutrient influx. Also, the other mechanisms leading to nutrient mobilisation may have become less efficient, due, for example, to less intense biochemical weathering in a transport-limited weathering system (Stallard and Edmond, 1983), or to a progressively diminishing return flux of P from the sediments. As such, the phosphorus–oxygen negative feedback mechanism may have become stronger than the positive feedback mechanisms leading to enhanced P availability. This then may have resulted in an increase in

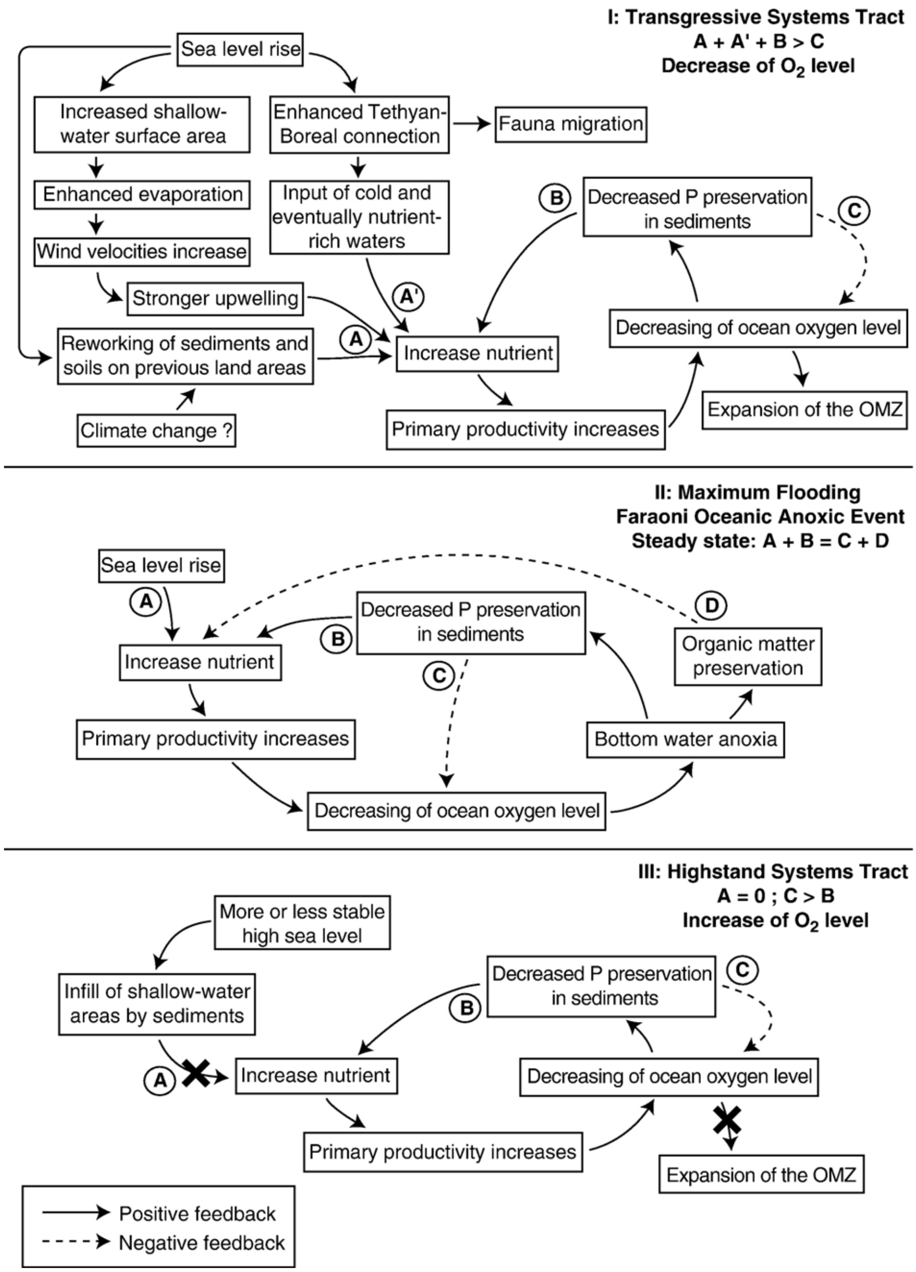

Fig. 8. Three-step (transgressive systems tract, maximum flooding, highstand systems tract) box model of the unfolding of the Faraoni event. See text for explanation.

oceanic oxygen levels, the diminution of the OMZ, and thus the termination of the oceanic anoxic conditions.

In this model, the Faraoni level is considered as the turning point during the evolution of this oceanic oxygen depletion event. Indeed, the increased transfer of organic matter into the sedimentary reservoir should be considered as the response of the Earth system by which it counteracts the decrease of oceanic oxygen levels.

5.5. The attenuated $\delta^{13}C$ signature during the late Hauterivian and early Barremian

One of the notable features of the Faraoni oceanic anoxic event is its poor expression in the $\delta^{13}C$ record. The $\delta^{13}C$ record of the late Hauterivian is characterized by a long-term steady increase of approximately 1‰ that culminates in a maximum near the Hauterivian–Barremian boundary, followed by a small decrease in the earliest Barremian (van de Schootbrugge et al., 2000; Godet et al., 2006). Unlike the oceanic anoxic events of the Valanginian, early Aptian and latest Cenomanian, the Faraoni anoxic event is not related to a well-expressed positive excursion in $\delta^{13}C$. The accumulation of organic-rich sediments accompanied by an episode of carbonate platform drowning is an expression of important changes in the carbon cycle that normally would find an expression in the $\delta^{13}C$ record. Either the Faraoni anoxic event is the result of regional, rather than global, environmental change limited to the Tethyan realm and the changes in the carbon household within this realm were not sufficiently important to influence global $\delta^{13}C$ signatures, or a buffering mechanism capable of attenuating the $\delta^{13}C$ record played a role. This buffering mechanism may have been related to different mechanisms, such as the enhanced productivity of shallow-water carbonates outside the western tethyan realm or the increased size of the oceanic dissolved inorganic carbon reservoir (e.g., van de Schootbrugge et al., 2003; Bartley and Kah, 2004).

5.6. The carbonate platform drowning episode during the latest Hauterivian and early Barremian: consequence of the Faraoni event?

The Faraoni oceanic anoxic event is contemporaneous with the onset of a platform drowning event along the northern tethyan margin that started during the latest Hauterivian and ended near the boundary between the early and late Barremian (D3 in Föllmi et al., 1994). Interestingly, the time covered by this drowning episode is mirrored by contrasting variations in PAR in the Western Tethys, i.e. by a negative shift associated with the late Hauterivian Faraoni event and by two major positive shifts during the early Barremian. These two latter peaks in PAR may reflect an increase of nutrient input induced by change towards probably more humid climate in the western tethyan realm. These climate changes and related changes in nutrient input came after the Faraoni oceanic anoxic event and may have prolonged the drowning episode, the onset of which is related to the environmental changes during the Faraoni event. Subsequently, during the late Barremian platform growth took up again, leading to the deposition of the "Urgonian" limestone that was promoted to a large extent by photozoans. The unfolding of this important phase in the evolution of helvetic platform growth may have been related to an overall decrease in P availability as is documented by our P-accumulation curve.

6. Conclusions

Monitoring phosphorus accumulation in pelagic and hemi-pelagic sediments of the western Tethys during the late Hauterivian and Barremian allows us to better understand the associated palaeoceanographic changes and especially the unfolding of the late Hauterivian Faraoni oceanic anoxic event. Our results correlate well with those obtained by van de Schootbrugge et al. (2003) for the late Hauterivian. Good correlation is also seen with the DSDP–ODP-based curve of Föllmi (1995).

Based on the general evolution of the PAR curve and its correlation with inferred sea-level variations, we propose a new model for the origin of the Faraoni event that incorporates increased nutrient mobilization on the continent and an improved tethyan–boreal connection that is linked to a positive feedback loop generated by a decrease in the capacity of phosphorus preservation in the sedimentary reservoir and a negative feedback loop related to changes in the ocean oxygen cycle.

Moreover, the Faraoni event is linked to the onset of an important platform drowning event along the northern tethyan margin. An extended increase in nutrient input during the early Barremian may have extended the drowning episode well into the Barremian.

Finally, during the late Barremian, the recorded low PAR values are in agreement with the worldwide development of the Urgonian facies, reflecting oligotrophic conditions on the shelf.

Acknowledgments

The authors acknowledge Rodolfo Coccioni, Pascal Linder, Haydon Mort, Claire Rambeau, Virginie Matera and Philipp Steinmann for their help in the field and/or stimulating discussions. Special thanks go to the team of the "Reserve Géologique de Haute-Provence" for providing an authorization for fieldwork. We thank Helmut Weissert and an anonymous reviewer for their critical reviews. Financial support from the Swiss National Science Foundation Project 2100-067807/1 and 200020-105206/1 is gratefully acknowledged.

References

Anderson, L.D., Delaney, M.L., 2000. Sequential extraction and analysis of phosphorus in marine sediments: streamlining of the SEDEX procedure. Limnology and Oceanography 45 (2), 509–515.

Anderson, L.D., Delaney, M.L., Faul, K.L., 2001. Carbon to phosphorus ratios in sediments: implications for nutrient cycling. Global Biogeochemical Cycles 15 (1), 65–79.

Bartley, J.K., Kah, L.C., 2004. Marine carbon reservoir, C_{org}–C_{carb} coupling, and the evolution of the Proterozoic carbon cycle. Geology 32 (2), 129–132.

Baudin, F., Bulot, L.G., Cecca, F., Coccioni, R., Gardin, S., Renard, M., 1999. Un équivalent du "Niveau Faraoni" dans le bassin du Sud-Est de la France, indice possible d'un événement anoxique fini-hauterivien étendu à la Téthys méditerranéenne. Bulletin de la Société Géologique de France 170 (4), 487–498.

Behar, F., Beaumont, V., Penteado, H.L.D., 2001. Rock-Eval 6 technology: performances and developments. Oil and Gas Science and Technology 56 (2), 111–134.

Benitez-Nelson, C.R., 2000. The biogeochemical cycling of phosphorus in marine systems. Earth-Science Reviews 51 (1–4), 109–135.

Bréhéret, J.-G., 1994. The Mid-Cretaceous organic-rich sediments from the Vocontian zone of the French Southeast basin. In: Mascle, A. (Ed.), Hydrocarbon and Petroleum Geology of France, Special Publication of the European Association of Petroleum Geoscientists, vol. 4, pp. 295–320.

Broecker, W.S., Peng, T.-H., 1982. Tracers in the Sea. Lamont–Doherty Geological Observatory, Columbia University. Eldigio Press, Palisades, New-York. 690 pp.

Busnardo, R., 1965. Le stratotype du Barrémien. Mémoires du Bureau de Recherche Géologiques et Minières 34, 101–116.

Busnardo, R., Charollais, J., Weidmann, M., Clavel, B., 2003. Le Crétacé inférieur de la Veveyse de Châtel (Ultrahelvétique des Préalpes externes; canton de Fribourg, Suisse). Revue Paléobiology, Genève 22 (1), 1–174.

Cecca, F., Marini, A., Pallini, G., Baudin, F., Begouen, V., 1994. A guide-level of the uppermost Hauterivian (Lower Cretaceous) in the pelagic succession of Umbria–Marche Apennines (Central Italy): the Faraoni Level. Rivista Italiana di Paleontologia e Stratigrafia 99, 551–568.

Cecca, F., Faraoni, P., Marini, A., Pallini, G., 1995. Field-trip across the representative sections for the Upper Hauterivian–Barremian ammonite biostratigraphy in the Maiolica exposed at Monte Nerone, Monte Petrano and Monte Catria (Umbria–Marche, Apennines). Memorie Descrittive della Carta Geologica d'Italia 51, 187–211.

Coccioni, R., Baudin, F., Cecca, F., Chiari, M., Galeotti, S., Gardin, S., Salvini, G., 1998. Integrated stratigraphic, palaeontological, and geochemical analysis of the uppermost Hauterivian Faraoni Level in the Fiume Bosso section, Umbria–Marche Apennines, Italy. Cretaceous Research 19 (1), 1–23.

Colman, A.S., Holland, H.D., 2000. The global diagenetic flux of phosphorus from marine sediments to the oceans; redox sensitivity and the control of atmospheric oxygen levels. In: Glenn, C.R., Prévôt-Lucas, L., Lucas, J. (Eds.), Marine Authigenesis; From Global to Microbial, SEPM Special Publication, vol. 66, pp. 53–75.

Compton, J., Mallinson, D., Glenn, C.R., Filippelli, G.M., Föllmi, K.B., Shields, G., Zanin, Y., 2000. Variations in the global phosphorus cycle. In: Glenn, C.R., Prévôt-Lucas, L., Lucas, J. (Eds.), Marine Authigenesis; From Global to Microbial, SEPM Special Publication, vol. 66, pp. 21–33.

Delaney, M.L., 1998. Phosphorus accumulation in marine sediments and the oceanic phosphorus cycle. Global Biogeochemical Cycles 12 (4), 563–572.

Delanoy, G., 1997. Biostratigraphie des faunes d'ammonites à la limite Barrémien-Aptien dans la région d'Angles-Barrême-Castellane. Annales du Muséum d'Histoire Naturelle de Nice (Nice), tome XII, 1–270.

Eaton, A.D., Clesceri, L.S., Greenberg, A.E., 1995. Standard Methods for the Examination of Water and Wastewater (19th edition).

Emeis, K.-C., Struck, U., Leipe, T., Pollehne, F., Kunzendorf, H., Christiansen, C., 2000. Changes in the C, N, P burial rates in some Baltic Sea sediments over the last 150 years – relevance to P regeneration rates and the phosphorus cycle. Marine Geology 167, 43–59.

Erba, E., Channell, J.E.T., Claps, M., Jones, C.E., Larson, R.L., Opdyke, B., Premoli-Silva, I., Riva, A., Salvini, G., Torriceli, S., 1999. Integrated stratigraphy of the Cismon APTICORE (Southern Alps, Italy): a "reference section" for the Barremian–Aptian interval at low latitudes. Journal of Foraminiferal Research 29 (4), 371–391.

Fiet, N., Gorin, G., 2000. Lithological expression of Milankovitch cyclicity in carbonate-dominated, pelagic, Barremian deposits in central Italy. Cretaceous Research 21 (4), 457–467.

Filippelli, G.M., Delaney, M.L., 1995. Phosphorus geochemistry, diagenesis, and mass balances of the Miocene Monterey Formation at Shell Beach, California. U.S. Geological Survey Bulletin, G1–G11.

Filippelli, G.M., Delaney, L.M., 1996. Phosphorus geochemistry of equatorial Pacific sediments. Geochimica et Cosmochimica Acta 60 (9), 1479–1495.

Föllmi, K.B., 1995. 160 m.y. record of marine sedimentary phosphorus burial: coupling of climate and continental weathering under greenhouse and icehouse conditions. Geology 23, 859–862.

Föllmi, K.B., 1996. The phosphorus cycle, phosphogenesis and marine phosphate-rich deposits. Earth-Science Reviews 40 (1–2), 55–124.

Föllmi, K.B., Weissert, H., Bisping, M., Funk, H., 1994. Phosphogenesis, carbon-isotope stratigraphy, and carbonate-platform evolution along the Lower Cretaceous northern Tethyan margin. Geological Society of America Bulletin 106 (6), 729–746.

Föllmi, K.B., Tamburini, F., Hosein, R., Van de Schootbrugge, B., Arn, K., Rambeau, C., 2004. Phosphorus, a servant faithful to Gaia? Biosphere remediation rather than regulation. In: Schneider, S.H., Miller, J.R., Crist, E., Boston, P.J. (Eds.), Scientist Debate Gaia: The Next Century, pp. 79–92.

Funk, H., 1969. Typusprofile der helvetischen Kieselkalk Formation und der Altmann Schichten. Eclogae Geologicae Helvetiae 62 (1), 191–203.

Gale, A.S., Smith, A.B., Monks, N.E.A., Young, J.A., Howard, A., Wray, D.S., Huggett, J.M., 2000. Marine biodiversity through the late Cenomanian–Early Turonian: palaeoceanographic controls and sequence stratigraphic biases. Journal of Geological Society of London 157, 745–757.

Giraud, F., Beaufort, L., Cotillon, P., 1995. Contrôle astronomique de la sédimentation carbonatée dans le Crétacé inférieur du Bassin vocontien (SE France). Bulletin de la Société Géologique de France 166 (4), 409–421.

Godet, A., Bodin, S., Föllmi, K.B., Vermeulen, J., Gardin, S., Fiet, N., Adatte, T., Berner, Z., Stüben, D., van de Schootbrugge, B., 2006. Evolution of marine stable carbon-isotope record during the early Cretaceous: a focus on the late Hauterivian and Barremian in the Tethyan realm. Earth and Planetary Science Letters.

Gradstein, F.M., Ogg, J.G., Smith, A.G., Bleeker, W., Lourens, L.J., 2004. A new Geologic Time Scale with special reference to Precambrian and Neogene. Episodes 27 (2), 83–100.

Haq, B.U., Hardenbol, J., Vail, P.R., 1987. Chronology of fluctuating sea levels since the Triassic. Science 235, 1156–1167.

Hardenbol, J., Thierry, J., Farley, M.B., de Graciansky, P.-C., Vail, P.R., 1998. Mesozoic and Cenozoic sequence chronostratigraphic framework of European basins. In: de Graciansky, P.-C., Hardenbol, J., Jacquin, T., Vail, P.R. (Eds.), Mesozoic and Cenozoic Sequence Stratigraphy of European Basins, Special Publication Society for Sedimentary Geology, pp. 3–13.

Hay, W.W., DeConto, R., Wold, C.N., Wilson, K.M., Voigt, S., Schulz, M., Wold-Rossby, A., Dullo, W.-C., Ronov, A.B., Balukhovsky, A.N., Soeding, E., 1999. Alternative global Cretaceous paleogeography. In: Barrera, E., Johnson, C. (Eds.), The Evolution of Cretaceous Ocean/Climate Systems, Geological Society of America Special Paper, p. 332.

Herrle, J.O., 2002. Paleoceanographic and paleoclimatic implications on Mid-Cretaceous black shale formation in the Vocontian basin and the Atlantic: evidence from calcareous nannofossils and stable isotopes. Mikropaläontologische Mitteilungen 27, 1–113.

Hilbrecht, H., Frieg, C., Troger, K.-A., Voigt, S., Voigt, T., 1996. Shallow water facies during the Cenomanian–Turonian anoxic event: bio-events, isotopes, and sea level in southern Germany. Cretaceous Research 17, 229–253.

Holland, H.D., 1994. The phosphate–oxygen connection. Eos Trans. AGU 75 (3) (Ocean Sci. Meet. Suppl.: 96).

Ingall, E., Jahnke, R., 1994. Evidence for enhanced phosphorus regeneration from marine sediments overlain by oxygen depleted waters. Geochimica et Cosmochimica Acta 58 (11), 2571–2575.

Ingall, E.D., Jahnke, R., 1997. Influence of water-column anoxia on the elemental fractionation of carbon and phosphorus during sediment diagenesis. Marine Geology 139, 219–229.

Ingall, E.D., Bustin, R.M., Van Cappellen, P., 1993. Influence of water column anoxia on the burial and preservation of carbon and phosphorus in marine shales. Geochimica et Cosmochimica Acta 57 (2), 303–316.

Iruthayaraj, M.R., Morachan, Y.B., 1978. Relationship between evaporation from different evaporimeters and meteorological parameters. Agricultural Meteorology 19 (2–3), 93–100.

Jarvis, I., Mabrouk, A., Moody, R.T.J., de Cabrera, S., 2002. Late Cretaceous (Campanian) carbon isotope events, sea-level change and correlation of the Tethyan and Boreal realms. Palaeogeography, Palaeoclimatology, Palaeoecology 188 (3–4), 215–248.

Jenkyns, H.C., 1999. Mesozoic anoxic events and palaeoclimate. Zentralblatt Geologie und Paläontologie 1 (Heft 7–9), 943–949.

Jenkyns, H.C., 2003. Evidence for rapid climate change in the Mesozoic–Palaeogene greenhouse world. Philosophical Transactions of the Royal Society, London, A 361, 1885–1916.

Jenkyns, H.C., Gale, A.S., Corfield, R.M., 1994. Carbon- and oxygen-isotope stratigraphy of the English Chalk and Italian Scaglia and its palaeoclimatic significance. Geological Magazine 131, 1–34.

Jones, C.E., Jenkyns, H.C., 2001. Seawater strontium isotopes, oceanic anoxic events, and seafloor hydrothermal activity in the Jurassic and Cretaceous. American Journal of Science 301, 112–149.

Lenton, T.M., Watson, A.J., 2000. Redfield revisited: 2. What regulates the oxygen content of the atmosphere? Global Biogeochemical Cycles 14 (1), 249–268.

Lini, A., Weissert, H., Erba, E., 1992. The Valanginian carbon isotope event; a first episode of greenhouse climate conditions during the Cretaceous. Terra Nova 4 (3), 374–384.

Mutterlose, J., Bornemann, A., 2000. Distribution and facies patterns of Lower Cretaceous sediments in northern Germany: a review. Cretaceous Research 21 (6), 733–759.

Redfield, A.C., 1958. The biological control of chemical factors in the environment. American Scientist 46, 205–222.

Reimers, C., Kastner, M., Garrison, R.E., 1990. The role of bacterial mats in phosphate mineralization with particular reference to the Monterey Formation. In: Burnett, W.C., Riggs, S.R. (Eds.), Phosphate Deposits of the World, vol. 3. Neogene to Modern Phosphorites. Cambridge University Press, Cambridge, pp. 300–311.

Ruttenberg, K.C., 1992. Development of a sequential extraction method for different forms of phosphorus in marine sediments. Limnology Oceanography 37 (7), 1460–1482.

Ruttenberg, K.C., 1993. Reassessment of the oceanic residence time of phosphorus. Chemical Geology 107 (3–4), 405–409.

Schlanger, S.O., Jenkyns, H.C., 1976. Cretaceous oceanic anoxic events: causes and consequences. Geologie en Mijnbouw 55, 179–184.

Schlanger, S.O., Arthur, M.A., Jenkyns, H.C., Scholle, P.A., 1987. The Cenomanian–Turonian oceanic anoxic event: I. Stratigraphy and distribution of organic-rich beds and the marine ^{13}C excursion. In: Brooks, J., Fleet, A.J. (Eds.), Marine Petroleum Sources Rocks, Geological Society, London, Special Publications, pp. 371–399.

Slomp, C.P., Thomson, J., de Lange, G.J., 2004. Controls on phosphorus regeneration and burial during formation of eastern Mediterranean sapropels. Marine Geology 203 (1–2), 141–159.

Stallard, R.F., Edmond, J.M., 1983. Geochemistry of the Amazon: 2. The influence of geology and weathering environment on the dissolved load. Journal of Geophysical Research 88, 9671–9688.

Tamburini, F., Huon, S., Steinmann, P., Grousset, F.E., Adatte, T., Föllmi, K.B., 2002. Dysaerobic conditions during Heinrich events 4 and 5: evidence from phosphorus distribution in a North Atlantic deep-sea core. Geochimica et Cosmochimica Acta 66 (23), 4069–4083.

Tamburini, F., Föllmi, K.B., Adatte, T., Bernasconi, S.M., Steinmann, P., 2003. Sedimentary phosphorus record from the Oman margin: new evidence of high productivity during glacial periods. Paleoceanography 18 (1), 1015.

Trümpy, R., 1960. Paleotectonic evolution of the Central and Western Alps. Bulletin of the Geological Society of America 71, 843–908.

Tyrrell, T., 1999. The relative influences of nitrogen and phosphorus on oceanic primary production. Nature 400, 525–531.

Van Cappellen, P., Ingall, E.D., 1996. Redox stabilization of the atmosphere and oceans by phosphorus-limited marine productivity. Science 271, 493–496.

Van de Schootbrugge, B., Föllmi, K.B., Bulot, L.G., Burns, S.J., 2000. Paleoceanographic changes during the Early Cretaceous (Valanginian–Hauterivian): evidence from oxygen and carbon stable isotopes. Earth and Planetary Science Letters 181, 15–31.

Van de Schootbrugge, B., Kuhn, O., Adatte, T., Steinmann, P., Föllmi, K.B., 2003. Decoupling of P- and C_{org}-burial following Early Cretaceous (Valanginian–Hauterivian) platform drowning along the NW Tethyan margin. Palaeogeography, Palaeoclimatology, Palaeoecology 199 (3–4), 315–331.

Vermeulen, J., 1980. Etude de la famille des Pulchelliidae, révision de trois espèces types du Barrémien du Sud-Est de la France, Thèse de Doctorat de Spécialité, Nice. 101 pp.

Vermeulen, J., 2002. Etude stratigraphique et paléontologique de la famille des Pulchelliidae (Ammonoidea, Ammonitina, Endemocerataceae). Géologie alpine, Grenoble, France. 333 pp.

Weissert, H., 1989. C-isotope stratigraphy, a monitor of paleoenvironmental change: a case study from the Early Cretaceous. Surveys in Geophysics 10, 1–61.

Weissert, H., Erba, E., 2004. Volcanism, CO_2 and palaeoclimate; a Late Jurassic–Early Cretaceous carbon and oxygen isotope record. Journal of the Geological Society of London 161 (4), 695–702.

Weissert, H., Lini, A., Föllmi, K.B., Kuhn, O., 1998. Correlation of Early Cretaceous carbon isotope stratigraphy and platform drowning events: a possible link? Palaeogeography, Palaeoclimatology, Palaeoecology 137, 189–203.

Wissler, L., Weissert, H., Masse, J.-P., Bulot, L.G., 2002. Chemostratigraphic correlation of Barremian and lower Aptian ammonite zones and magnetic reversals. International Journal of Earth Sciences (Geol. Rundsch.) 91, 272–279.

Wissler, L., Weissert, H., Buonocunto, F.P., Ferreri, V., D'Argenio, B., 2004. Calibration of the Early Cretaceous time scale: a combined chemostratigraphic and cyclostratigraphic approach to the Barremian–Aptian interval, Campania Apennines and Southern Alps (Italy). In: D'Argenio, B., Fischer, A.G., Premoli-Silva, I., Weissert, H., Ferreri, V. (Eds.), Cyclostratigraphy: Approach and Case Histories, SEPM Special Publication, vol. 81, pp. 123–133.